Supporting Information

Schmidt et al. 10.1073/pnas.1103318108

SI Materials and Methods

Animals. Male C57/Bl6N mice (Charles River Laboratories) were used for all experiments. Animals were kept on a 12 light:12 dark cycle (lights on at 6:00 AM); food and water was provided ad libitum. The experiments were carried out in accordance with European Communities Council Directive 86/609/EEC. All efforts were made to minimize animal suffering during the experiments. The protocols were approved by the committee for the Care and Use of Laboratory Animals of the Government of Upper Bavaria, Germany.

Experimental Design. *Maternal separation.* Separation took place in a separate room in the animal facility as described previously (1, 2). The initiation day of maternal separation for all experiments was postnatal day 8. If a nest was assigned to maternal separation, mothers were removed from their home cages between 8:00 and 10:00 AM. The home cage, containing the litter, was then placed for 24 h on a heating pad maintained at 30–33 °C. Neither food nor water was available during the separation period. Nonseparated litters remained undisturbed with their mothers.
Food deprivation. The animals were placed in a new cage without access to food between 8:00 and 10:00 AM, 24 h before testing. Water was available ad libitum at all times.
Dexamethasone treatment. Between 8:00 and 10:00 AM, animals were injected s.c. with 10 mg/kg dexamethasone (Ratiopharm) or vehicle (saline). After the injection, the animals remained undisturbed in their home cage until the time of testing.
RU486 treatment. For glucocorticoid receptor (GR) antagonist treatment, animals were injected twice s.c. with 100 mg/kg RU486 (Sigma) or vehicle (polyethylene glycol) 16 and 8 h before sacrifice.
Sampling. After decapitation, brains were removed, frozen in isopentane at −40 °C, and stored at −80 °C for in situ hybridization. For immunohistochemistry, animals were deeply anesthetized with ketamin/rompun and perfused intracardially with 4% paraformaldehyde. Brains were removed, postfixed overnight in 4% paraformaldehyde following overnight incubation in 20% sucrose solution at 4 °C, and then stored at −80 °C.

In Situ Hybridization and Immunohistochemistry. For in situ hybridization, frozen brains were sectioned in a cryostat microtome at 18 μm, thaw-mounted on superfrost plus slides (Menzel), dried, and kept at −80 °C. In situ hybridization using ^{35}S UTP-labeled ribonucleotide probes was performed as described previously (3, 4). The antisense cRNA hybridization probe was 486 bp long, covering exons 1–4 (forward primer: GTGGAGGGAAGGAGAAGGAC; reverse primer: TCCCGGACTTTGATGAACTC).

For immunohistochemistry, serial free-floating sections at 30 μm were cut and kept in cryoprotection solution at −20 °C. All of the following steps were interposed by repeated washes in PBS, and all reagents were diluted in PBS unless otherwise specified. After incubation in 0.2% Triton-X 100, 1 h blocking in 5% normal goat serum was performed. Incubation with the polyclonal rabbit–anti-DRR1 (1:200) and chicken–anti-GFP (1:1,000, Abcam) antibodies was performed for 24 h at 4 °C, followed by 1 h incubation at 4 °C with AlexaFluor 555 anti-rabbit and AlexaFluor 488 anti-chicken (1:200, Invitrogen). Sections were rinsed in distilled water, mounted on superfrost plus slides, and covered with Vectashield mounting medium (Vector) containing DAPI. For avidin–biotin–diaminobenzidine immunohistochemistry, the Vectastain ABC kit (Vector Laboratories) was used according to the manufacturer's instructions.

DNA Constructs. To construct plasmids expressing murine DRR1 in mammalian cells, murine cerebellum cDNA was used as a template for PCR reactions. PCR products were cloned downstream of the CMV promoter of the vector pRK5-SV40-MCS. To create FLAG-tagged versions of DRR1, the reverse primer contained the sequence for the tag. Primers for cloning were DRR1-For (TGCCTCCTCGAGCCTCCATGTACTCAGAGA), DRR1-Rev (GGCAGAAGCTTGATGGAGGGAGCTCTACAG), and DRR1-FLAG-Rev (GCAGAAGCTTGCTCACTTGTCATCGTCGTCCTTGTAGTCCAGTGCTCTTTCCTCGCTGGT).

For cloning plasmids encoding for GFP-tagged, His-tagged, or MBP-tagged proteins, inserts of DRR1 were subcloned from pRK5-S40-MCS vector into pEGFP-N1 vector (Clontech), pProEx-HT vector (Invitrogen), and pMAL vector (New England BioLabs), respectively. Details of the cloning strategy are available on request.

Cell Culture, Transfection, and Immunoprecipitation. Cultivation and transfection of human NIH 3T3, HEK, HeLa, and Neuro2a cells were as described previously (5, 6). For immunoprecipitation of overexpressed DRR1, HEK cells were transfected using electroporation with 10 μg of plasmid expressing FLAG-tagged DRR1. After 2 d of cultivation, the cells were solubilized in 1 mL of lysis buffer [20 mM Tris·HCl (pH 7.5), 130 mM NaCl, 20 mM Na_2MoO_4, 1 mM EDTA, 10% glycerol, 0.5% Triton X-100, 1:100 protease inhibitor mixture P2714 from Sigma]. The extract was incubated for 1 h on ice and centrifuged for 10 min at 13,000 × *g*/min, and then the protein concentration was determined. Lysates (1.5 mg) were incubated with the anti-FLAG M2 affinity gel from Sigma (A2220) overnight at 4 °C. Beads were treated as recommended by the manufacturer. The next day, the beads were washed three times with lysis buffer without Triton X-100, and samples were eluted with 100 μg/mL FLAG-peptide (Sigma) in 1× Tris-buffered saline. For immunoprecipitation of recombinantly expressed DRR1, 25 μg DRR1-FLAG-MBP or recombinant FLAG-BAP (Sigma) as control was added to lysate from untransfected cells.

Eluates were separated by SDS/PAGE on 12 or 15% acrylamide gels. Gels were stained with colloidal Coomassie brilliant blue G (Sigma). Coprecipitated protein bands were excised and analyzed by tandem mass spectrometry as described previously (7). Immunodetection was performed as described previously (8).

Bioinformatics. The computational analysis of glucocorticoid response elements (GRE)-binding sites conserved across species was performed with the MatInspector (9) and the Dialign TF program (Genomatix). In addition, a more stringent IUPAC pattern search was carried out using the palindromic GRE motif WGWACA$(N)_{1-5}$TGTWCW (W = A/T). For the alignment of the human and mouse DRR1 protein sequence, the program Clustal X version 2.0.9 (10) with default parameter settings was applied.

GRE in Vitro Analysis. Plasmid (10 μg) coding for FLAG-tagged GR was transfected into HEK 293 cells by electroporation (350 V, 700 μF; BioRad), and cells were cultivated for 3 d. Proteins were extracted by using lysis buffer A′, and FLAG-GR was bound to anti-FLAG agarose beads as described previously (11). Beads with immobilized GR were washed three times with protein–DNA-binding buffer (6), split equally according to the number of binding reactions in each experiment, and then incubated with 150 fmol ^{32}P-labeled GRE-containing double-

stranded oligonucleotide, 1 μg poly-deoxyinosine-deoxycytidine, 10 nM cortisol, in 100 μL binding buffer per reaction supplemented with 150 pmol of competitor oligonucleotides, where indicated, and incubated for 15 min. After two washings with protein–DNA-binding buffer, the bound oligonucleotides were eluted with high salt (50 μL of 700 mM NaCl), and radioactivity was determined.

Primary Hippocampal Neurons and Transfections. Preparation of primary neuronal cerebellum cultures derived from BL6 mice was based on Bayatti et al. (12). P1 animals were used for cultures. Cerebellum was dissected in HBSS, 7 mM Hepes (pH 7.4) at 4 °C, and then incubated in 0.1% Trypsin–PBS at 37 °C for 20 min. Brain structures were washed in MEM (20% horse serum, HS) and dissociated in an MEM (10% HS) through a 80-μm nylon mesh. Cells were seeded in MEM (10% HS, 1% pyruvate, 0.5% gentamycin). After 24 h, the media was changed to Neuro Basal A supplemented with 2% B27, 0.5% gentamycin, and 0.5 mM glutamin.

Primary hippocampal neurons derived from 18-d-old rat embryos were cultured as described (13). Neurons were transfected before plating with the Amaxa Nucleofector system (Lonza) using highly purified DNA (EndoFree Maxi Prep, Qiagen) as described (13). As control, neurons were transfected with pEGFP-N2 (Clontech). Mature neurons were transfected with Lipofectamine 2000 (Invitrogen) at 17 d in vitro (DIV). Briefly, DNA (1.2 μg/well) was mixed with 4 μL Lipofectamine in 200 μL glia-conditioned N2 medium, incubated for 30 min, and then added to a coverslip with neurons in a 12-well plate. After 2.5 h in the incubator, the neurons were washed with warm HBSS and put back in a glia-conditioned dish. Cells were analyzed 2 d later at 19 DIV.

Neuro2a Differentiation and Neuronal Polarization of Hippocampal Neurons. To determine the outgrowth of neurite-like structures in Neuro2a cells, 75,000 cells were seeded in a six-well plate (~7,900 cells/cm^2) and cultured overnight before transfection using six equivalents ExGen (Fermentas), as recommended by the manufacturer. For serum withdrawal, media was changed 24 h after transfection to DMEM containing 0.1 or 0.2% FCS, sodium pyruvate, and antibiotics. Pictures of live cultures were taken using a Fluorescence microscope (Olympus IX50). Length of neurites was determined manually using ImageJ software (National Institutes of Health). Cells with neurites were defined as cells having neurites of about the size of the cell soma. Development of hippocampal neurons transfected with DRR-GFP or the control vector pEGFP-N2 was analyzed after 2 DIV. Neurons were classified into cells without neurites (stage 1), cells with neurites with a length of at least two times the diameter of the cell body (stage 2), and cells with an axon with the longest neurite at least ~80 μm (stage 3) (14).

Immunofluorescence. NIH 3T3, HeLa, or N2A cells were seeded on poly-D-lysine and laminin or fibronectin-coated glass coverslips and transfected using ExGene as described above. For immunofluorescence of NIH 3T3, HeLa, and N2A cells or of primary murine neuronal cultures, cells were fixed with 4% paraformaldehyde in PBS for 20 min at room temperature (RT). Cells were extracted with 0.1% Triton X-100 for 10 min and blocked with 10% goat serum or 2% BSA in PBS. To stain primary hippocampal neurons from rat, cells were fixed with 4% paraformaldehyde and 4% sucrose in PBS for 20 min, quenched with 50 mM ammonium chloride in PBS for 10 min, and extracted with 0.1% Triton X-100 in PBS for 5 min. Coverslips were blocked in 2% FBS, 2% BSA, and 0.2% fish gelatin in PBS for the DRR1 staining. For staining of actin filaments, cells were incubated with 100 nM AlexaFluor 546 phalloidin (Invitrogen), Cy3 phalloidin (Cytoskeleton), or rhodamine phalloidin (Invitrogen) for 20 min at RT. For immunostaining, antibodies were diluted in PBS 0.1% Triton X-100. Images were recorded digitally using a fluorescence microscope (Axioplan 2 imaging, Zeiss) or a laser scanning microscope (Zeiss LSM 510 META NLO and Olympus LSM FV-1000). To determine the percentage of cells in apoptosis, cell were counted manually using ImageJ.

Correlation Analysis of Colocalizations. Quantitative assessments of the colocalizations of DRR1 with actin and synapsin were performed using MetaMorph software, version 7.7 (Molecular Devices). Maximum projections of *z*-stacks were used. Background correction was performed by linear subtraction of the average signal from areas with no cells (NIH 3T3; Fig. 2 and Fig. S2) or by applying medium filter 64 × 64 pixels with a subsample ratio of 1 (primary neurons, Fig. 4 *A* and *B*). The resulting image was converted to an 8-bit image (scaling minimum to maximum intensity values), and correlation plots were derived for the entire image and for 3–10 regions per cell (NIH 3T3 cells) or per image (primary neurons). Sizes of the defined regions were 50 × 50 pixels (NIH 3T3 cells), 25 × 25 pixels (primary neurons, colocalization of DRR1 with actin), or 20 × 20 pixels (primary neurons, colocalization of DRR1 with synapsin) to adjust for the different dimensions of the structures under investigation. Correlation values (Pearson's coefficient) were obtained for each subregion. As control, correlation values were obtained after turning the DRR1 image by 90°.

F-Actin Quantification in Cells. Neuro2a or NIH 3T3 cells were seeded (6,000 and 10,000 cells/well) on lysine (100 μg/mL in dH_2O 2 h at RT)- and laminin (10 μg/mL in dH_2O 2 h at RT)-coated coverslips in 24-well plates and transfected with 1 μg plasmid DNA using ExGene (six equivalents) in DMEM containing 10% FCS, 1% pyruvate, and antibiotics. After 6 h, the medium was renewed, and 24 h after transfection the medium was changed to high (10%) or low (0.1%) FCS-containing media. Forty-eight hours after transfection, the cells were fixed with 4% paraformaldehyde in PBS and extracted with 0.1% Triton X-100 for 10 min at RT. Cells were blocked with 10% goat serum in PBS for 1 h at RT. To visualize F-actin, cells were stained with 165 nM fluorescent–phalloidin (AlexaFluor 545 phalloidin, Invitrogen) for 20 min at RT, counterstained with DAPI (5 μg/mL in PBS) for 15 min at RT, and mounted in Pro Long Gold antifade media (Invitrogen).

Fluorescent images were taken using an epifluorescence microscope (Axioplan 2 imaging, Zeiss) and a 10× lens at a resolution of 1 μm/pixel and 16 bit. In each experiment, the same imaging parameters were used for one fluorescent channel to compare fluorescence intensities between different conditions. Single-cell analysis of actin and GFP fluorescence were acquired using the ImageJ software package (National Institutes of Health). The DAPI fluorescence images were thresholded and converted to a binary image. To obtain a single-cell mask, the binary image was processed (commands: erode, open, 2× dilate), and a particle analysis was performed (size: 0–1,000; circularity: 0.5–1). The regions of interest from the mask were used to measure the mean gray value in a fluorescent image of a single cell. Cells with a GFP fluorescence below 10,000 were assumed to be untransfected. See Fig. S4*E* for a sample analysis.

Cell Viability Assay. For measuring cell viability using 3-(4,5-Dimethylthiazol-2-yl)-2,5-diphenyltetrazolium bromide (MTT), HEK-293, or Neuro2a cells have been transfected using ExGene as described above and cultured for 48 h in 10% FCS containing media. MTT has been added to a final concentration of 0.5 mg/mL and incubated at 37 °C for 5 h. MTT crystals have been solubilized by adding equal volumes of solubilization solution (5% SDS, 50% dimethylformamide, pH 4.1) and by incubating at

4 °C overnight. The dye produced was measured by absorption at 630 nm in a Spectrophotometer (DU 640; Beckman).

Immunogold and Electron Microscopy. A naive mouse was perfused with 4% paraformaldehyde, 0.05% glutaraldehyde, and 0.2% picric acid in 0.1 M phosphate buffer (pH 7.4). Slices ~500 μm thick were cut from the dorsal hippocampus and slam-frozen on a liquid nitrogen-cooled copper mirror followed by freeze substitution in methanol at −85 °C in a Leica AFS2. The slices were infiltrated and embedded in Lowicryl before polymerization under ultraviolet light at −50 °C.

Ultrathin sections of 70-nm thickness were cut on a Leica UCT ultramicrotome and collected on formvar-coated nickel slot grids. Excess aldehyde groups were treated with 0.05 M glycine for 15 min at RT, and nonspecific binding was blocked by 5% BSA, 0.1% cold-water fish gelatin, and 5% normal goat serum in 0.01 M PBS (pH 7.4) for 15 min at RT. Sections were incubated with 30-μL droplets of 0.5% BSA, 0.1% cold-water fish gelatin, and 1% normal goat serum in 0.01 M PBS (pH 7.4) for two sets of 5 min at RT. The grids were transferred to drops of a mixture of primary antibodies containing 1:50 rabbit anti-DRR1 and 1:500 mouse antisynaptophysin in PBS with 0.5% BSA and 0.1% cold-water fish gelatin in a humidified box overnight at 4 °C. The grids were washed in PBS and then in deionized water before fixation in 2% glutaraldehyde in PBS for 5 min. After washing, the grids were counterstained with uranyl acetate and lead citrate and examined in a JEM 1400 transmission electron microscope, and digital images were captured with an AMT XR60.

Antibodies. Rabbit polyclonal antibodies targeting DRR1 were produced by BioGenes using histidine-tagged DRR1-FLAG in immunization buffer (see below) and affinity-purified using the same antigen.

For immunstainings/immunoblots mouse antisynapsin (Synaptic Systems), mouse anti-MAP2 (AP10; Sigma), chicken anti-neurofilament H (Chemicon/Millipore), rabbit anti-Prx1 (PAb; Alexis), goat anti-Prx1 (N14, Santa Cruz), rabbit anticleaved caspase-3 (Cell Signaling), goat anti-actin (I-19; Santa Cruz), chicken anti-GFP (Abcam), mouse anti-GFP (Santa Cruz), mouse anti-FLAG (M2; Sigma). For immunogold staining, mouse anti-synaptophysin MAB 5258 from Chemicon was used. The secondary antibodies used were Alexa Fluor 488/546/555/647 goat anti-rabbit IgG (Invitrogen), Alexa Fluor 488/546 goat anti-mouse IgG (Invitrogen), Alexa Fluor 488 goat anti-chicken IgG (Invitrogen), Cy3 donkey anti-chicken IgG (Dianova), HRP goat anti-rabbit IgG (Sigma), HRP goat anti-mouse IgG (Sigma), and HRP bovine anti-goat IgG (Santa Cruz).

Recombinant Proteins. Histidine-tagged DRR1 was expressed in pBL3Lys bacteria (Invitrogen) induced by 1 mM isopropyl β-D-1 thiogalactopyranoside (IPTG) for 3 h at 37 °C. Lysis was performed under denaturing conditions in buffer containing 100 mM NaH_2PO_4 (pH 8.0), 10 mM Tris, and 8 M urea. Purification was performed using HisTrap HP columns (GE Healthcare). For binding, lysates were mixed in a 1:1 ratio with native lysis buffer containing 50 mM NaH_2PO_4 (pH 8.0), 300 mM NaCl, and 20 mM imidazole before applying to the column. The column was washed using native lysis buffer, complemented with 50 mM imidazole, and eluted with 500 mM imidazole. The eluates were concentrated and buffer was exchanged to immunization buffer (1 M urea, 1 mM EDTA, 2 mM DTT, 300 mM NaCl, 0.1% SDS, 10% glycerol) using PD10 sephadex columns (GE Healthcare).

It was not possible to purify histidine-tagged DRR1 stably under native conditions. We therefore used DRR1 fused to maltose-binding protein (MBP) to express DRR1 under native conditions. Biochemical analyses were performed with MBP-DRR1-FLAG fusion protein because DRR1-FLAG appeared to be unstable at 4 °C in assay buffer when cleaved off the MBP (using FactorXa). MBP-DRR1-FLAG was expressed in pBL3Lys bacteria induced by 0.2 mM IPTG for 2 h at 37 °C and purified using amylose–agarose (New England BioLabs) and then FLAG-agarose (Sigma) according to the manufacturer's recommendations. The bacterial pellets were lysed by the freeze–thaw method in a dry-ice ethanol bath and then resuspended in column buffer [10 mM Tris (pH 7.4), 200 mM NaCl, and 1 mM EDTA, supplemented with protease inhibitor mixture and 1 mg/mL lysozyme], incubated for 1 h on ice, and then sonicated. The lysates were cleared by centrifugation (20,000 rpm/48,400 × *g*; Beckman Avanti J-25, rotor JA-20) and then filtered through a 0.22-μM syringe filter. Lysates were applied on amylose resins by gravity flow and washed with column buffer (CB: 10 mM Tris (pH 7.4), 200 mM NaCl, 1 mM EDTA), and the protein was eluted using 10 mM maltose in CB. The amylose eluate was applied directly on FLAG-agarose beads (Sigma) equilibrated with CB. The FLAG-agarose was washed with 5 mM Tris (pH 8.0) before eluting elution with 1× FLAG-peptide (100 μg/mL in 5 mM Tris, pH 8.0). Eluates were concentrated using Centricon columns (Millipore YM-50, cutoff 50 kDa or GE Healthcare Vivaspin 2, cutoff 30 kDa). Protein concentration and purity were determined by SDS/PAGE followed by Coomassie staining.

F-Actin Cosedimentation. For cosedimentation assay of actin filments, nonmuscle actin from human platelets (Cytoskeleton #APHL99) in general actin buffer (GAB) [5 mM Tris·HCl (pH 8.0), 0.2 mM $CaCl_2$, 0.2 mM ATP, 0.5 mM DTT] were formed in vitro by addition of 1/10th volume of 10× filament-promoting buffer (FAB) (500 mM KCl, 20 mM $MgCl_2$, 10 mM ATP) and by incubation for 1 h at 25 °C in a thermal cycler (Peqlab). MBP-DRR1-FLAG (10 μL) in 5 mM Tris (pH 8.0) were added to 40 μL of filaments and incubated for 30 min at 25 °C. Actin filaments were separated from unpolymerized monomers by ultracentrifugation for 1.5 h with 34,000 rpm/150,000 × *g* at 25 °C (Beckman LB-70M, SW60Ti rotor with microcentrifuge tubes and adapters). For filament breakdown assays, 1 mg/mL actin filaments were formed as for the cosedimentation assay and then diluted with GAB. Immediately after dilution, 10 μL MBP-DRR1-FLAG were added to 40 μL of diluted F-actin and incubated at 25 °C for 1 h. For breakdown of bundled filaments, 8 μM actin was polymerized in 1× FAB for 1.5 h at RT. The preformed filaments were then mixed with 2.4 μM MBP-DRR1-FLAG or MBP as control in 5 mM Tris (pH 8.0) (6 μM actin and 0.6 μM DRR1 or MBP during bundling) and incubated for 30 min at RT. Breakdown was induced by diluting actin bundles with 1× GAB to the final actin concentration indicated and by incubating for 1.5 h at RT. F-actin was separated from G-actin by ultracentrifugation as described above and the percentage of F-actin values was determined by densitometric analysis of Coomassie-stained gels using a calibrated densitometer (GS800; Bio-Rad).

Pyrene–Actin Assay. The rate of actin polymerization was measured by monitoring the change in fluorescence intensity of pyrene-labeled actin at 407 nm (excitation at 365 nm) in a fluorescence spectrometer (Genius Pro, Tecan: excitation filter 340-nm bandwidth, 30 nm; emission filter 410-nm bandwidth, 10 nm). Freshly thawed pyrene-labeled rabbit skeletal muscle actin (Cytoskeleton #AP05) and unlabeled human nonmuscle β-actin (>99% pure, Cytoskeleton #APHL99) were each diluted in GAB [5 mM Tris·HCl (pH 8.0), 0.2 mM $CaCl_2$, 0.2 mM ATP, 0.5 mM DTT] to a concentration of 1 mg/mL. Labeled and unlabeled G-actin were mixed in a ratio of 1:10 and incubated overnight at 4 °C. The mixture was precleared by centrifugation at 150,000 × *g* for 1 h at 4 °C and then diluted in GAB before use in the assay. Polymerization reactions containing 60 μL of pyrene–actin mixtures and 20 μL of test proteins in 5 mM Tris (pH 8.0) were preincubated for 10 min at 25 °C. The reactions were

then initiated by adding 20 μL of 2.5× FAB (diluted from 10× FAB in GAB). The final concentration of actin in the reaction was 4 μM. To visualize the slope as representation of the speed of F-actin formation, the first derivative of the reactions was calculated using the GraphPad Prism 5.0 software (smoothed using 25 neighbors and a sixth-order smoothing polynomial).

F-Actin Visualization in Vitro. Fluorescently labeled actin filaments were visualized by total internal reflection (TIRF) microscopy (Olympus TIRF M2 Excellence System) at the Light Microscopy Facility of the Deutsches Zentrum für Neurodegenerative Erkrankungen. This system is based on an IX81 microscope stand, and TIRF illumination is achieved by the motorized integrated TIRF illumination combiner (TIR-MITICO). Alexa Fluor-568–labeled actin was imaged using a 561 laser, a quadband dichroic, and an mCherry emission filter. Images were acquired with an EMCCD camera through an UAPON 100× TIRF objective with NA of 1.49. Olympus CellR software was used for TIRF angle adjustment and acquisition.

For TIRF analysis, the in vitro actin polymerization was initiated by addition of polymerization buffer [final concentration: 2 mM $MgCl_2$, 50 mM KCl, 1 mM ATP, 1 mM EGTA, 50 mM DTT, 0.5% (wt/vol) methylcellulose] to 1 μM G-actin in GAB [5 mM Tris·HCl (pH 8.0), 0.2 mM $CaCl_2$, 0.2 mM ATP, 0.5 mM DTT] at 25 °C. The proportion of Alexa Fluor-568–labeled actin was 20%. After 2 h of polymerization at 25 °C, different molar ratios of DRR1 to actin or buffer only were added as indicated to the preformed actin filaments. After the indicated time points, this solution was transferred to a glass coverslip before microscopic examination.

Fluorescence microscopy of phalloidin-labeled actin filaments was based on Blanchoin et al. (15). Unlabeled or partially pyrene-labeled actin filaments (8 μM) from pyrene–actin assay after 2 h of polymerization at 25 °C with 0.3× concentration FAB were fixed with equal amounts of Alexa Fluor 546-phalloidin for 10 min at 25 °C and diluted to a final concentration of 10 nM in fluorescence buffer containing 10 mM imidazole (pH 7.0), 50 mM KCl, 1 mM $MgCl_2$, 100 mM DTT, 1 mM EGTA, 100 μg/mL glucose oxidase (Sigma), 3 mg/mL glucose, 20 μg/mL catalase (Sigma), and 0.5% methylcellulose (4000 centipoise; Sigma). Two microliters of the reaction was applied to poly-D-lysine–coated coverslips and viewed with a fluorescence microscope (Zeiss, Axioplan 2).

Viral Overexpression of DRR1. For viral overexpression of DRR1 in the hippocampus, we used an adeno-associated bicistronic AAV1/2 vector (http://www.GeneDetect.com) containing the CAG-DRR1-IRES-EGFP-WPRE-BGH-polyA expression cassette (containing coding sequence of DRR1 NCBI CCDS ID CCDS26813.1). For the control group, we used the same vector construct expressing only EGFP. Virus production, amplification, and purification were performed by Genedetect.

Viral DRR1 overexpression was performed as described previously (2). Briefly, 12-wk-old mice were anesthetized with isoflurane, and 1 μL of either AAV-DRR1 or AAV-EGFP (titres: 1.3 × 1,012 genomic particles/mL) were bilaterally injected in the dorsal hippocampus at 0.06 μL/min by glass capillaries with tip resistance of 2–4 MΩ in a stereotactic apparatus. The following coordinates were used: 1.7 mm posterior to bregma, 1.8 mm lateral from midline, and 1.8 mm below the surface of the skull (16). After surgery, mice were treated for 5 d with Metacam via drinking water. Behavioral testing started 4 wk after virus injection.

Electrophysiology. Male control (n = 6) and DRR1 overexpressing (n = 6) mice were decapitated, and their brains were removed rapidly and placed in ice-cold artificial cerebrospinal fluid (ACSF) containing (in mM): 125 NaCl, 2.5 KCl, 25 $NaHCO_3$, 2 $CaCl_2$, 1 $MgCl_2$, 25 D-glucose, 1.25 NaH_2PO_4 (pH 7.4) after equilibration with carbogen (95% O_2/5% CO_2). Coronal slices containing the dorsal hippocampus (350 μm thick) were prepared using a vibroslicer. Afterward, the slices were incubated for 30 min at 34 °C and subsequently stored at room temperature (23–25 °C) for at least 90 min. For experimentation, slices were placed in a submerged recording chamber and continuously superfused with ACSF at a flow rate of 3 mL/min. Square-pulse electrical stimuli (0.066 Hz, 1–6 V, 50 μs) were delivered via a bipolar tungsten electrode (insulated to the tip, 50-μm diameter) that was positioned within the stratum radiatum of the CA1 region. All recordings were performed at room temperature, low-pass-filtered at 1 kHz, and digitized at 5 kHz. Evoked field excitatory postsynaptic potential (fEPSPs) were recorded using glass microelectrodes (~1 MΩ open-tip resistance) that were filled with ACSF and also positioned within the CA1 stratum radiatum. For long-term potentiation (LTP) and paired pulse facilitation measurements, the stimulus intensities were adjusted in a manner to produce an fEPSP of ~50% of the amplitude at which a population spike becomes clearly observable. LTP was induced by high frequency stimulation (HFS, 100 stimuli at 100 Hz). From every animal, two to three slices were used for the experiments. The paired-pulse ratio was calculated as fEPSP2 amplitude/fEPSP1 amplitude.

Quantitative Neuromorphology. After decapitation, the brains were rapidly removed and immersed in 50 mL of Golgi–Cox solution for 14 d. Thereafter, brains were dehydrated and embedded in 8% celloidin. Serial transverse 150-μm sections were collected, mounted on glass slides, and processed using a modified Golgi–Cox protocol (17, 18). Spine densities of the following types of neurons were quantified at 400× using a computer-based neuron tracing system (Neurolucida; MicroBrightField): (*i*) apical dendrites of CA1 pyramidal neurons and (*ii*) apical dendrites of CA3 pyramidal neurons. For the CA1 region, an overall of 30 dendritic segments of 20-μm length per animal were analyzed from the medial and terminal parts of the apical dendrites. In the CA3 region, dendritic spine density was calculated by tracing a part of the apical dendrite from its origin to the terminal segments. All protrusions, thin or stubby, with or without terminal bulbous expansions, were counted as spines if they were in direct continuity with the dendritic shaft. The average spine density (number of visible spines per micrometer of dendritic length) was calculated by dividing the number of counted spines by the length of the analyzed dendritic segments. All measurements were done by an experimenter blind to the experimental conditions of the animals.

Behavioral Analysis. All behavioral testing took place in the same room where the animals were habituated for at least 1 wk and was performed during the light phase between 7:00 and 12:00 AM All tests were recorded and analyzed using a video-tracking system (Anymaze 4.20, Stoelting).

Y-maze. The Y-maze was made of gray PVC and consisted of three evenly illuminated arms (30 × 10 × 15 cm, 30 lx) with an angle of 120° between each of the two arms. The apparatus was surrounded by various spatial cues. To ensure that the mice had sufficient spatial cues available without having to stretch up and look outside of the maze, we also introduced intramaze cues (triangles, bars, and plus signs), which served the same purpose as the external cues. The Y-maze test comprises two trials separated by an intertrial interval (ITI) to assess spatial recognition memory. During the first trial (the acquisition phase), the mouse was allowed to explore only two of the three arms for 10 min while the third arm was blocked. After 15, 30, or 60 min ITI, the second trial (the retrieval phase) was conducted during which all three arms were accessible for 5 min. The percentage of time spent in the novel arm compared with the known arms was scored using a video-tracking system (Anymaze 4.20; Stoelting)

with a significantly higher percentage than chance level (33.3%) rated as successful spatial memory. Between tests and animals the apparatus was thoroughly cleaned to exclude olfactory cues as orientation markers.

Morris water maze. The test was performed according to Morris (19) with some adaptations for mice. Briefly, a circular pool (100 cm in diameter) was filled with 21 + 1 °C water that was made opaque by the addition of chalk. A platform (9 cm in diameter) was placed inside the pool 1 cm below the surface of the water (spatial training) or 1 cm above the surface during visual training. Several extramaze visual cues were attached to the walls of the experimental room, at a distance of approximately 50–100 cm from the pool. After habituation of the mice to the maze in a 1-min free swim trail, the animals were trained with four trials to find a visible platform (visual training). During the spatial training phase, the animals had to perform four trials each on 3 consecutive days, where the now-submerged and not-visible platform remained in a constant position. The intertrail interval was 10 min. On the following day, a probe trial was performed in which the platform was removed and the animals were allowed to explore the maze for 1 min. On the final day, the cognitive flexibility of the animals was tested in a four-trial reversal learning task, where the animals had to acquire a different location on the platform. Latency to reaching the platform, path length, and location of the animal was analyzed using a video-tracking system (Anymaze 4.20; Stoelting).

Open field test. Open field arenas (50 × 50 × 50 cm) were made of gray PVC and evenly illuminated during testing (20 lx). General locomotor activity was recorded for 15 min (distance traveled) using a video-tracking system (Anymaze 4.20; Stoelting) and virtually divided into three distinct intervals.

Spatial object relocation task. The test was performed in the above described open field arenas according to Palchykova et al. (20). The open field arenas were surrounded by various spatial cues. The animals were habituated to the empty open field arenas for 10 min on 2 consecutive days before testing. To test memory for the spatial location of objects, the open field arena was equipped with two identical copies of an object (aluminum cube, 5 × 5 × 5 cm) placed 5 cm apart from the arena walls in two adjacent corners. During the acquisition trials, mice were allowed to explore the experimental context two times for 10 min separated by 15 min ITI. During the 5-min retrieval trial, 30 min following the last acquisition trial, one object remained in its original location (nondisplaced object) and the other object was placed in the opposite corner (displaced object). The location of the displaced object was counterbalanced among animals. Mice that remembered the original spatial location of the objects were expected to prefer the displaced object to the nondisplaced object. Object exploration was scored only when the mouse's nose or front paws were in direct contact with the object. Between tests and animals the apparatus and the objects were thoroughly cleaned to exclude olfactory cues as orientation markers.

Home cage activity. Home cage activity was recorded as described previously using a home cage activity counter (21). Briefly, the system consisted of a tilting platform (4 × 170 × 250 mm) on which the empty home cage was orientated in balance. Each time the animal crossed the centerline of the cage, the platform tipped slightly to the other side. An electronic switch underneath the platform was thereby activated, and tilting events were counted. The margin of the platform movement was reduced to a minimum, so that the animal was not disturbed in its behavior. Locomotion measurement started at 6:00 AM at the onset of the light phase; 12 h later, at the beginning of the dark phase, the number of counts was recorded and the counter was reset. At 6:00 AM, the number of counts during the dark phase was recorded.

Statistical Analysis. The commercially available program SPSS 12 was used for statistical analysis. Simple group comparisons were performed using the two-tailed unpaired *t* test. If more than two groups were compared, an ANOVA was performed followed by Bonferroni post hoc analysis. The level of significance was set at $P < 0.05$. All data are presented as mean ± SEM.

1. Liebl C, et al. (2009) Gene expression profiling following maternal deprivation: Involvement of the brain renin-angiotensin system. *Front Mol Neurosci* 2:1.
2. Monory K, et al. (2006) The endocannabinoid system controls key epileptogenic circuits in the hippocampus. *Neuron* 51:455–466.
3. Schmidt MV, Oitzl MS, Levine S, de Kloet ER (2002) The HPA system during the postnatal development of CD1 mice and the effects of maternal deprivation. *Brain Res Dev Brain Res* 139:39–49.
4. Schmidt MV, et al. (2007) Persistent neuroendocrine and behavioral effects of a novel, etiologically relevant mouse paradigm for chronic social stress during adolescence. *Psychoneuroendocrinology* 32:417–429.
5. Abel GA, et al. (2002) Activity of the GR in G2 and mitosis. *Mol Endocrinol* 16: 1352–1366.
6. Schmidt U, et al. (2003) Essential role of the unusual DNA-binding motif of BAG-1 for inhibition of the glucocorticoid receptor. *J Biol Chem* 278:4926–4931.
7. Rüegg J, Holsboer F, Turck C, Rein T (2004) Cofilin 1 is revealed as an inhibitor of glucocorticoid receptor by analysis of hormone-resistant cells. *Mol Cell Biol* 24: 9371–9382.
8. Wochnik GM, et al. (2005) FK506-binding proteins 51 and 52 differentially regulate dynein interaction and nuclear translocation of the glucocorticoid receptor in mammalian cells. *J Biol Chem* 280:4609–4616.
9. Cartharius K, et al. (2005) MatInspector and beyond: Promoter analysis based on transcription factor binding sites. *Bioinformatics* 21:2933–2942.
10. Larkin MA, et al. (2007) Clustal W and Clustal X version 2.0. *Bioinformatics* 23:2947–2948.
11. Wochnik GM, et al. (2004) Inhibition of GR-mediated transcription by p23 requires interaction with Hsp90. *FEBS Lett* 560:35–38.
12. Bayatti N, Zschocke J, Behl C (2003) Brain region-specific neuroprotective action and signaling of corticotropin-releasing hormone in primary neurons. *Endocrinology* 144: 4051–4060.
13. Stiess M, et al. (2010) Axon extension occurs independently of centrosomal microtubule nucleation. *Science* 327:704–707. Available at http://www.ncbi.nlm.nih.gov/pubmed/20056854 (accessed Jan. 11, 2010).
14. Dotti CG, Sullivan CA, Banker GA (1988) The establishment of polarity by hippocampal neurons in culture. *J Neurosci* 8:1454–1468.
15. Blanchoin L, et al. (2000) Direct observation of dendritic actin filament networks nucleated by Arp2/3 complex and WASP/Scar proteins. *Nature* 404:1007–1011.
16. Franklin K (2008) *The Mouse Brain in Stereotaxic Coordinates* (Academic Press, New York), 3rd Ed.
17. Bock J, Gruss M, Becker S, Braun K (2005) Experience-induced changes of dendritic spine densities in the prefrontal and sensory cortex: Correlation with developmental time windows. *Cereb Cortex* 15:802–808.
18. Glaser EM, Van der Loos H (1981) Analysis of thick brain sections by obverse-reverse computer microscopy: Application of a new, high clarity Golgi-Nissl stain. *J Neurosci Methods* 4:117–125.
19. Morris R (1984) Developments of a water-maze procedure for studying spatial learning in the rat. *J Neurosci Methods* 11:47–60.
20. Palchykova S, Winsky-Sommerer R, Meerlo P, Dürr R, Tobler I (2006) Sleep deprivation impairs object recognition in mice. *Neurobiol Learn Mem* 85:263–271.
21. Ganea K, Liebl C, Sterlemann V, Müller MB, Schmidt MV (2007) Pharmacological validation of a novel home cage activity counter in mice. *J Neurosci Methods* 162: 180–186.
22. Lupas A, Van Dyke M, Stock J (1991) Predicting coiled coils from protein sequences. *Science* 252:1162–1164.

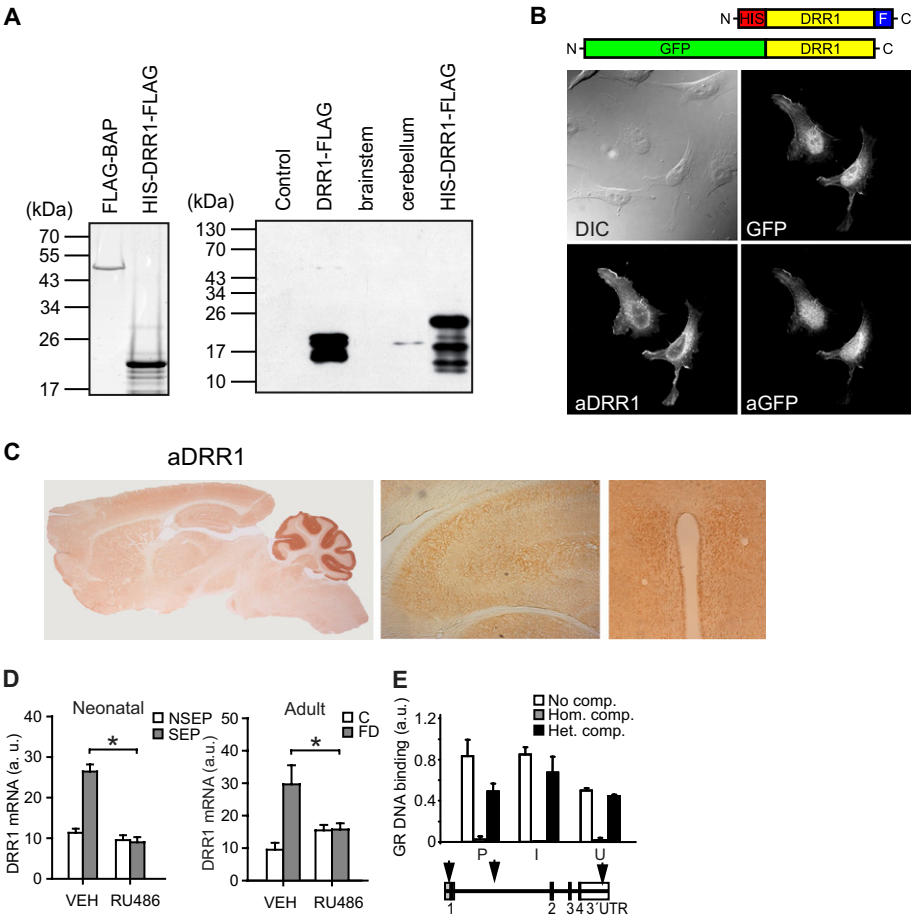

Fig. S1. Distribution of DRR1 in cells and tissue and proof of GR-dependent regulation. (*A*) (*Left*) To raise antibodies in rabbits, HIS-DRR1-FLAG was recombinantly expressed in bacteria and purified under denaturing conditions. Coomassie-stained gel shows purity of recombinant HIS-DRR1-FLAG. (*Right*) Immunoblot analysis using purified polyclonal DRR1 antibodies to evaluate antibody specificity in HEK293 cells overexpressing DRR1 (DRR1-FLAG) and to evaluate endogeneous DRR1 protein levels in extracts from different brain regions. Control, untransfected HEK293 cell lysate. (*B*) Immunostaining using DRR1 antibodies to test the ability of the antibodies to detect natively folded DRR1. (*Upper* panels) Schematic view of constructs used for immunization (HIS-DRR1-FLAG) and for verification in immunostaining (GFP-DRR1). (*Lower* panels) Immunstaining of HeLa cells transiently transfected with constructs expressing GFP-DRR1. DIC, differential interference contrast; GFP, fluorescence of the transfected GFP-DRR1 construct; aDRR1, immunostain with aDRR1 antibodies; aGFP, immunostain with aGFP antibodies (detected with secondary antibodies coupled to Alexa Fluor 546). aDRR1 antibodies lead to fluorescence only in transfected cells, with a pattern almost identical to GFP. (*C*) DRR1 protein expression in mouse brain slices analyzed by avidin–biotin–diaminobenzidine immunohistochemistry. (*D*) Treatment with the GR antagonist RU486 compared to vehicle (VEH) prevented stress-induced increase of *DRR1* mRNA in the paraventricular nucleus of neonatal (NSEP, nonseparated; SEP, maternal separation) and adult (C, control; FD, food deprivation) animals (neonates: condition—$F_{1,43} = 8.424$, $P = 0.006$; treatment—$F_{1,43} = 16.944$, $P = 0.000$; condition*treatment—$F_{1,43} = 4.831$, $P = 0.002$; adults: condition—$F_{1,25} = 21.360$, $P = 0.002$; condition*treatment—$F_{1,25} = 12.090$; $P = 0.002$). *, Significant compared to vehicle. (*E*) Validation of GR binding to in silico predicted GREs in the promoter (P), intron1 (I), and 3′UTR (U) of *DRR1*. Arrows indicate location of the GREs in the *DRR1* gene structure. Binding to radiolabeled oligonucleotides representing the respective GRE was done in the absence of competitor DNA (open bars) or in the presence of unlabeled homologous (gray bars) or heterologous (black bars) oligonucleotides.

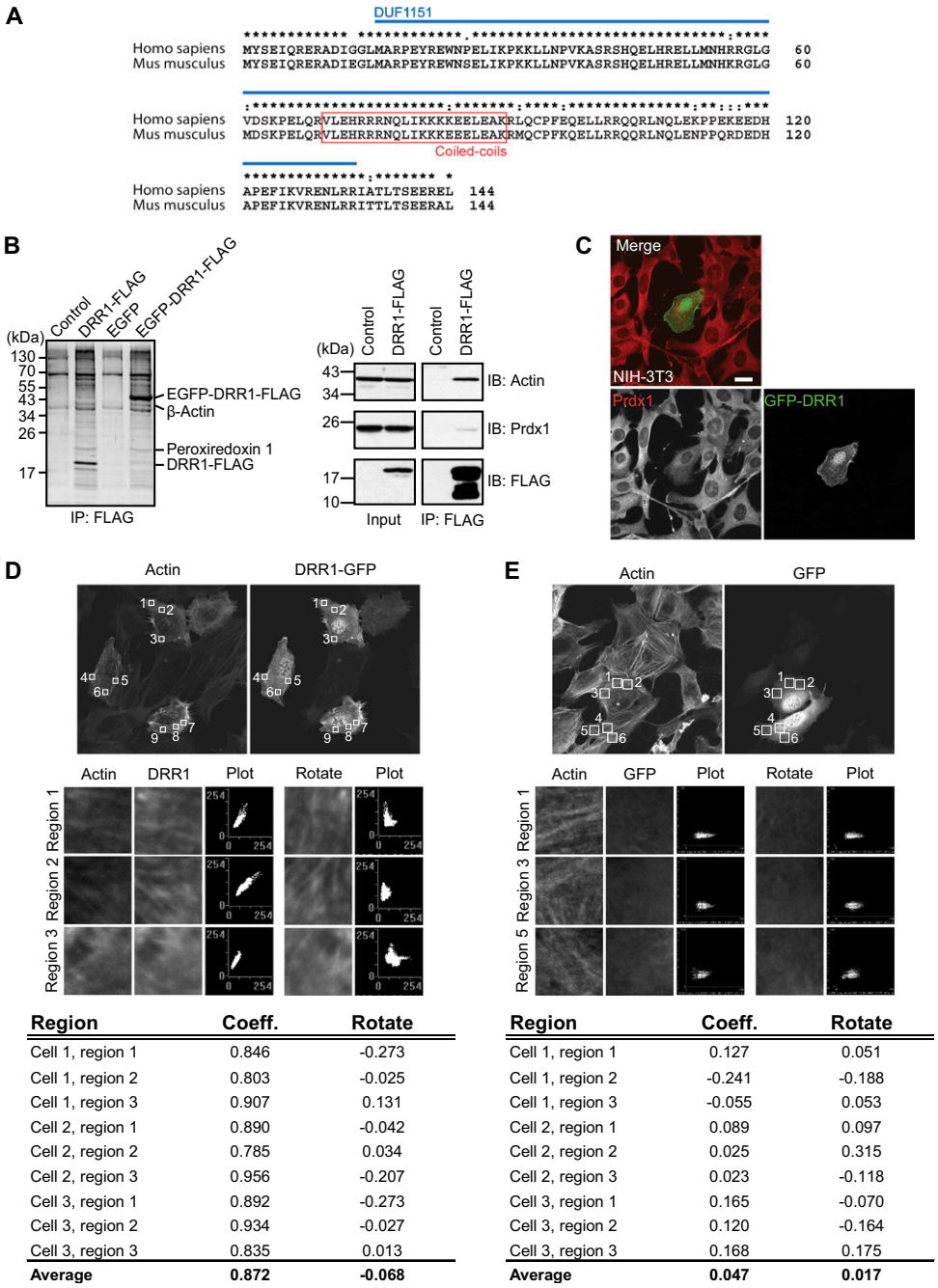

Region	Coeff.	Rotate
Cell 1, region 1	0.846	-0.273
Cell 1, region 2	0.803	-0.025
Cell 1, region 3	0.907	0.131
Cell 2, region 1	0.890	-0.042
Cell 2, region 2	0.785	0.034
Cell 2, region 3	0.956	-0.207
Cell 3, region 1	0.892	-0.273
Cell 3, region 2	0.934	-0.027
Cell 3, region 3	0.835	0.013
Average	**0.872**	**-0.068**

Region	Coeff.	Rotate
Cell 1, region 1	0.127	0.051
Cell 1, region 2	-0.241	-0.188
Cell 1, region 3	-0.055	0.053
Cell 2, region 1	0.089	0.097
Cell 2, region 2	0.025	0.315
Cell 2, region 3	0.023	-0.118
Cell 3, region 1	0.165	-0.070
Cell 3, region 2	0.120	-0.164
Cell 3, region 3	0.168	0.175
Average	**0.047**	**0.017**

Fig. S2. DRR1 protein interactions. (*A*) Human (accession no. O95990) and murine (accession no. Q78TU8) DRR1 amino acid sequences were aligned using the Clustal algorithm. Boxed area shows potential coiled coil region as being predicted by the COILS program (22). The UniProt server predicts a coiled coil region from aa 66 to aa 112 for the human sequence. Blue line indicates the protein domain of unknown function (DUF1151). Asterisks indicate amino acid residues that are conserved across both species, colons indicate strong similarity between human and murine protein, and dots indicate weak similarity. (*B*) FLAG-tagged DRR1 or FLAG- and EGFP-tagged DRR1 were expressed in HEK293 cells, precipitated from cell extracts using FLAG antibody beads. (*Left*) Coomassie-stained gel shows similar interaction profile of DRR1-FLAG and EGFP-DRR1-FLAG. (*Right*) Western blot analysis confirmed coprecipitation of actin and peroxiredoxin-1. (*C*) GFP-tagged DRR1 was expressed in NIH 3T3 cells, and after fixation the cells were immunostained for peroxiredoxin-1. (Scale, 25 μm.) (*D* and *E*) Colocalization analysis. DRR-GFP or GFP were expressed in NIH 3T3 cells, and after fixation cells were stained for F-actin using fluorescent phalloidin. Colocalization analysis was performed using the program Metamorph on defined regions (50 × 50 pixels) indicated by white boxes. Correlation values ("Coeff.") were obtained for each subregion. As control, correlation values were obtained after turning the DRR1-GFP or GFP image by 90° ("Rotate").

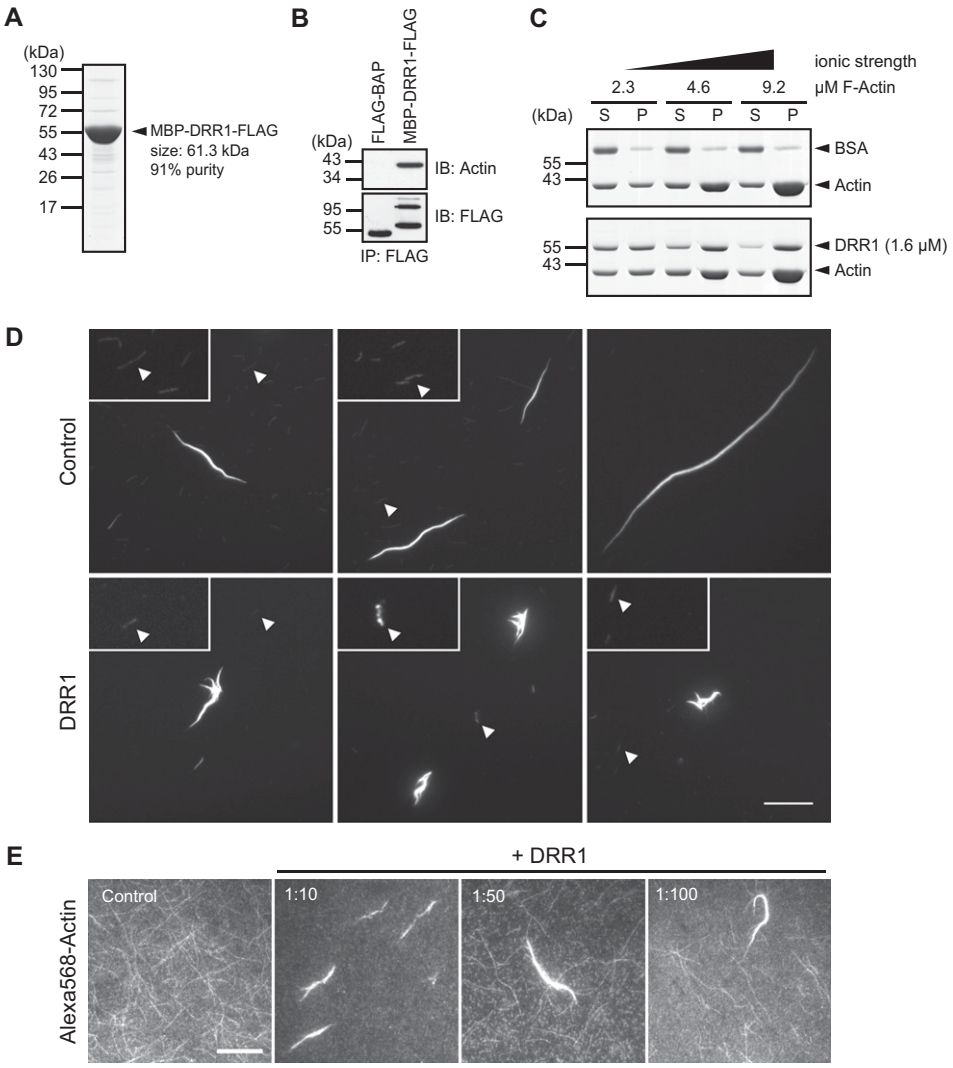

Fig. S3. DRR1 binds to, stabilizes, and bundles actin. (*A*) DRR1 was fused at the N terminus to MBP and at the C terminus to FLAG peptide, expressed in bacteria, and purified by tandem purification using first amylose–resin and then FLAG-agarose resin. (*B*) Incubation of the purified DRR1 or FLAG-BAP recombinant protein (Sigma) as control with protein extracts from HEK cells and immunoprecipitation with anti-FLAG agarose beads confirmed actin as an interaction partner. (*C*) Destabilization of preformed F-actin by dilution and lowering of the ionic strength revealed a stabilizing effect of DRR1 on F-actin in the pelletation assay at 2.3 μM actin (quantification displayed in Fig. 3*B*). S, supernatant. P, pellet. (*D*) DRR1 induces actin bundles. Fluorescence microscopy of F-actin visualized with Alexa Fluor 546–phalloidin. Actin (8 μM; 99% purity) was polymerized in the presence of 1.6 μM (0.1 μg/mL) purified DRR1 (*Lower* panels, three representative images) or 0.1 μg/mL BSA (*Upper* panels). Arrowheads indicate regions enlarged and brightened in the *Insets*. (*E*) TIRF microscopy of F-actin partially labeled with Alexa Flour 568–actin. Actin (1 μM; 95% purity) was polymerized in the presence of DRR1 with the indicated molar ratios (DRR1: actin). (Scale: *D* and *E*, 10 μm.)

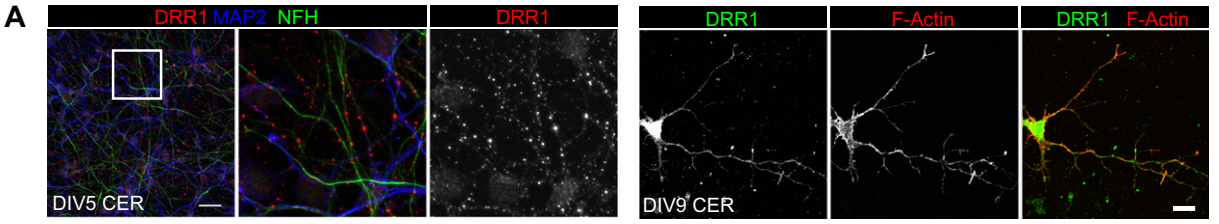

B Colocalization correlation - HIP: F-Actin vs. DRR1

Region	Coeff.	Rotate
Entire Image 1	0.734	
Image 1, region 1	0.810	-0.121
Image 1, region 2	0.773	-0.163
Image 1, region 3	0.788	0.132
Image 1, region 4	0.804	-0.034
Image 1, region 5	0.741	0.114
Entire Image 2	0.852	
Image 2, region 4	0.740	-0.061
Image 2, region 5	0.771	0.377
Entire Image 3	0.836	
Image 3, region 1	0.851	0.093
Image 3, region 2	0.885	0.042
Image 3, region 3	0.884	0.291
Image 3, region 4	0.895	0.116
Image 3, region 5	0.776	-0.140
Average	**0.813**	**0.021**

Colocalization correlation - HIP: Synapsin vs. DRR1

Region	Coeff.	Rotate
Entire Image 1	0.557	
Image 1, region 1	0.698	0.062
Image 1, region 2	0.638	0.094
Image 1, region 3	0.795	0.025
Image 1, region 4	0.575	0.017
Image 1, region 5	0.627	-0.093
Entire Image 2	0.512	
Image 2, region 1	0.513	0.046
Image 2, region 2	0.655	0.176
Image 2, region 3	0.630	0.026
Image 2, region 4	0.662	0.086
Image 2, region 5	0.586	0.033
Entire Image 3	0.459	
Image 3, region 1	0.647	0.082
Image 3, region 2	0.621	-0.150
Image 3, region 3	0.452	0.030
Image 3, region 4	0.653	-0.074
Image 3, region 5	0.089	0.154
Image 3, region 6	0.256	-0.121
Image 3, region 7	0.569	0.061
Image 3, region 8	0.282	0.117
Image 3, region 9	0.584	0.730
Image 3, region 10	0.387	0.168
Average	**0.546**	**0.073**

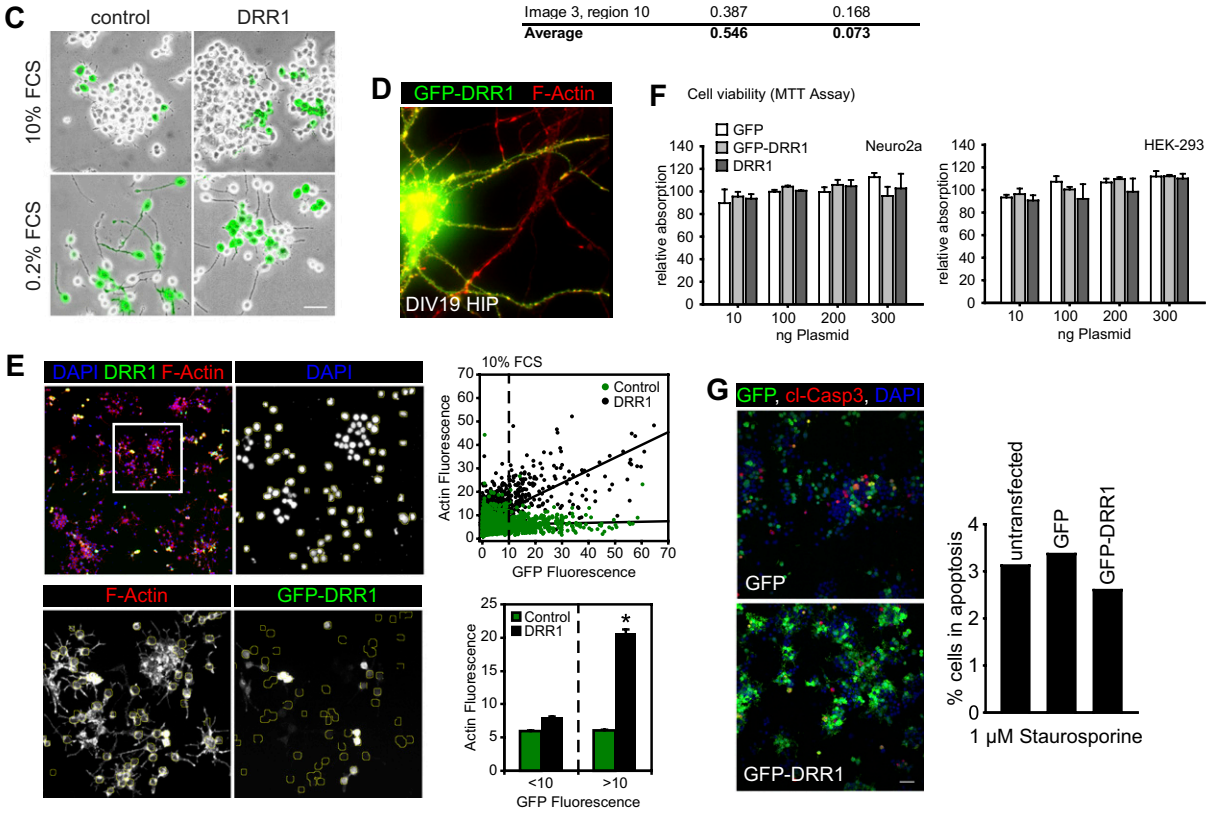

Fig. S4. DRR1 colocalizes with actin and interferes with neurite outgrowth. (*A*) Cerebellar neurons were cultivated for 5 d (*Left*) or 9 d (*Right*) and stained with DRR1 antibodies in combination with either antibodies against NFH and MAP2 to visualize axons and dendrites, respectively (*Left*) or with phalloidin to visualize actin (*Right*) and analyzed by laser scanning microscopy. (Scale: 25 μm.) (*B*) Colocalization analysis of DRR1 with F-actin (*Left*) or with synapsin (*Right*) in primary hippocampal neurons. Compare confocal images in Fig. 4*A* (actin) and Fig. 4*B* (synapsin). Colocalization analyses were performed on defined regions (25 × 25 pixels for actin; 20 × 20 pixels for synapsin) to adjust for the different dimensions of the structures under investigation. Correlation values ("Coeff.") were obtained for each subregion and the entire image. As a control, correlation values were obtained after turning the DRR1 image by 90 ° ("Rotate"). (*C*) N2A cells were transfected with either DRR1-GFP or GFP alone, and differentiation was induced by lowering the serum concentration. DRR1-transfected cells displayed significantly fewer neurites (quantification in Fig. 4*D*). (Scale: 50 μm.) (*D*) Primary hippocampal neurons were cultivated for 16 d, transfected with

Legend continued on following page

GFP-DRR1, and stained with phalloidin to visualize actin 3 d later. (*E*) F-actin quantification in DRR1-overexpressing cells. N2A cells, ectopically expressing GFP-DRR1 or GFP as control, were stained for F-actin using Alexa Fluor-545–phalloidin and DAPI to visualize cell nuclei. To measure actin and GFP fluorescence per cell in the epifluorescent images, the DAPI signal was used to create a single-cell mask (indicated by thin yellow outlines). (*Right* panels) Mean fluorescent intensities in the regions of interest (ROIs) of the GFP channel were plotted against the mean fluorescent intensities in the ROIs of the rhodamine (actin) channel. Cells with a GFP intensity above 10,000 (in a 16-bit image) were determined to be nontransfected. GFP-DRR1 overexpression in N2A cells cultivated in 10% FCS containing media led to a significant increase in F-actin and indicate a correlation of GFP-DRR1 expression and the F-actin signal [GFP-DRR1: 2,324 cells counted (8.82% of the cells with a GFP fluorescence >10), $R_2 = 0.4309$; EGFP: 1,629 cells counted (16.01% cells with a GFP fluorescence >10), $R_2 = 0.0037$; $P = 4.82 \times 10^{-58}$ (GFP/control vs. GFP-DRR1, >10)]. (*F*) Overexpression of DRR1 does not affect cell viability as measured in the MTT assay. N2A or HEK-293 cells were transfected with different amounts of plasmids coding for DRR1, DRR1-GFP, or GFP, as indicated. Cell viability was assessed by the MTT assay. (*G*) DRR1 overexpression does not increase apoptosis. HEK-293 cells were transfected with either GFP or GFP-DRR1. Cells were incubated with staurosporine, and apoptotic cells were stained with antibodies against cleaved caspase 3 (cl-Casp3). DAPI was used to stain DNA. The percentage of cells positive for cleaved caspase 3 was determined.

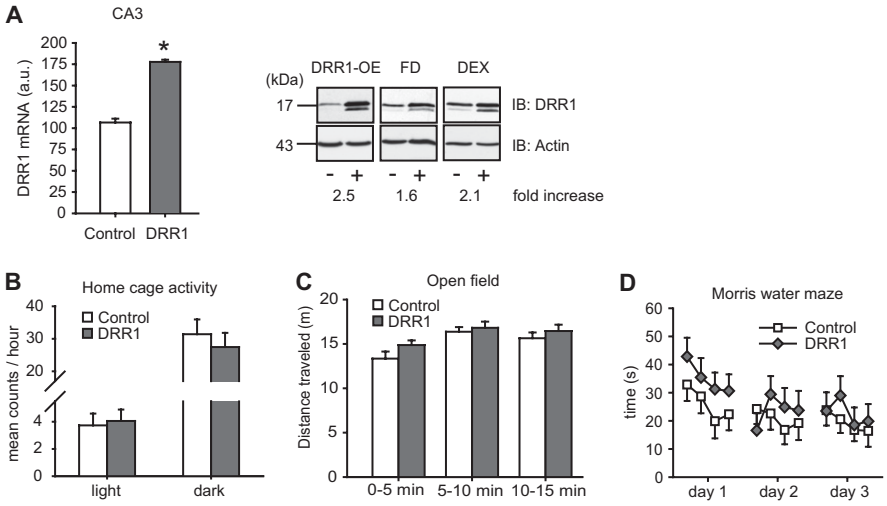

Fig. S5. DRR1 overexpressing mice. (*A*) (*Left*) DRR1 expression is significantly increased in the CA3 region of overexpressing animals compared with animals injected with the control virus (T22 = 13.760; $P = 0.0001$). (Right) Immunoblot comparison of the hippocampal DRR1 fold regulation induced by viral overexpression (OE), food deprivation (FD), or 12 h after dexamethasone treatment (DEX). (*B*) DRR1 overexpression in the hippocampus does not change locomotion in the home cage. (*C*) Expression of DRR1 has no effect on locomotor behavior in the open field. (*D*) DRR1 overexpression has no significant effect on performance in the Morris water maze during the acquisition training trials.